Since January 2020 Elsevier has created a COVID-19 resource centre with free information in English and Mandarin on the novel coronavirus COVID-19. The COVID-19 resource centre is hosted on Elsevier Connect, the company's public news and information website.

Journal of Clinical Virology 154 (2022) 105218

Contents lists available at ScienceDirect

Journal of Clinical Virology

journal homepage: www.elsevier.com/locate/jcv

Rapid and accurate identification of SARS-CoV-2 Omicron variants using droplet digital PCR (RT-ddPCR)

Margaret G. Mills [a,*], Pooneh Hajian [a], Shah Mohamed Bakhash [a], Hong Xie [a], Derrek Mantzke [a], Haiying Zhu [a], Garrett A. Perchetti [a], Meei-Li Huang [a], Gregory Pepper [a], Keith R. Jerome [a,b], Pavitra Roychoudhury [a,b], Alexander L. Greninger [a,b]

[a] Department of Laboratory Medicine and Pathology, Virology Division, University of Washington School of Medicine, Seattle, Washington, USA
[b] Vaccine and Infectious Disease Division, Fred Hutchinson Cancer Research Center, Seattle, Washington, USA

ARTICLE INFO

Keywords:
B.1.1.529
Allelic discrimination

ABSTRACT

Background: Some mutations in the receptor binding domain of the SARS-CoV-2 Spike protein are associated with increased transmission or substantial reductions in vaccine efficacy, including in recently described Omicron subvariants. The changing frequencies of these mutations combined with their differing susceptibility to available therapies have posed significant problems for clinicians and public health professionals.
Objective: To develop an assay capable of rapidly and accurately identifying variants including Omicron in clinical specimens to enable case tracking and/or selection of appropriate clinical treatment.
Study Design: Using three duplex RT-ddPCR reactions targeting four amino acids, we tested 419 positive clinical specimens from February to December 2021 during a period of rapidly shifting variant prevalences and compared genotyping results to genome sequences for each sample, determining the sensitivity and specificity of the assay for each variant.
Results: Mutation determinations for 99.7% of detected samples agree with NGS data for those samples, and are accurate despite wide variation in RNA concentration and potential confounding factors like transport medium, presence of additional respiratory viruses, and additional mutations in primer and probe sequences. The assay accurately identified the first 15 Omicron variants in our laboratory including the first Omicron in Washington State and discriminated against S-gene dropout Delta specimen.
Conclusion: We describe an accurate, precise, and specific RT-ddPCR assay for variant detection that remains robust despite being designed prior the emergence of Delta and Omicron variants. The assay can quickly identify mutations in current and past SARS-CoV-2 variants, and can be adapted to future mutations.

1. Background

The evolution of SARS-CoV-2 enabled by two-and-a-half years and over 500 million cases of human-to-human transmission has resulted in numerous mutations in the receptor binding domain (RBD) of the spike protein. This is the region that binds to the human cell receptor Angiotensin-converting enzyme 2 (ACE2) to enable viral invasion of the host cell [1–3] and it is the region targeted by most antibodies, both illness- and vaccine-derived [4,5]. Consequently, a number of the amino acid changes observed in the RBD of SARS-CoV-2 variants have been predicted or demonstrated to correlate with increased transmissibility and/or reduced plasma neutralization and vaccine efficacy [5–11], including N501Y, K417N/T, L452R, and E484K/Q/A. These RBD mutations were detected in a parade of lineages identified as Variants of Concern (VOC) or Interest (VOI) through the first half of 2021: Alpha (B.1.1.7, N501Y) [12–14]; Beta (B.1.351, K417N/E484K/N501Y) [15,16]; Gamma (P.1, K417T/E484K/N501Y) [17–19]; Delta (B.1.617.2 and AY.x, L452R) [20,21]; Kappa (B.1.617.1, L452R/E484Q) [22]; and more. Before the approval of vaccines against SARS-CoV-2, monoclonal antibodies (mAbs) were the primary tool available to protect patients from severe COVID-19 [23,24], and even with the availability of vaccines, mAbs remain important treatment options for vulnerable patients [25,26]. These drugs need to be administered within a limited time after infection in order to provide protection [26–28]. But because of the

* Corresponding author at: Dept of Lab Med and Pathology, Virology Division, University of Washington School of Medicine, 1616 Eastlake Ave E Suite 320, Seattle, WA, 98102, USA.
E-mail address: gracem@uw.edu (M.G. Mills).

https://doi.org/10.1016/j.jcv.2022.105218
Received 22 December 2021; Received in revised form 5 June 2022;
Available online 18 June 2022

kaleidoscope of RBD amino acid combinations presented by the circulating variants, because of the varying effectiveness with which different mAbs neutralize different variants [21,23,29,30], and because of the constantly changing frequencies of the variants themselves in different areas of the world, selection of mAb or mAb cocktail was challenging for large parts of 2021, prompting calls for clinical tests capable of rapidly identifying SARS-CoV-2 variant in clinical specimens. With the appearance and rise of the Omicron variant (B.1.1.529, K417N/E484A/G496S/Q498R/N501Y) [31] and subvariants (BA.x) this need is again growing [32–34].

2. Objective

Single nucleotide mutations, such as those encoding these amino acid changes, are challenging to identify with routine RT-PCR. Variant identification using larger changes elsewhere in the genome, such as the S-gene target failure (SGTF) used to identify both Alpha and Omicron variants, has been extremely useful for surveillance purposes by us and others [35–37], but is not accurate enough for making clinical decisions. Sequencing identifies mutations definitively, but not quickly enough to allow for treatment decisions.

Droplet digital (dd)PCR enables rapid and accurate genotyping of small-but-critical mutations [38–40]. Building on our earlier assay [36], we sought to develop an assay that could identify these key functional mutations in Spike, quickly enough to be of use to clinicians.

3. Study design

3.1. Sample extraction

Total nucleic acids were extracted from nasal/pharyngeal and nasal swabs using either Roche MagNA Pure 96 instrument and DNA & Viral NA Small Volume kit or ThermoFisher KingFisher according to manufacturer instructions. All MagNA Pure extractions used 200 µl of input volume and 100 µl elution; all KingFisher extractions used 200 µl input volume and 50 µl elution.

3.2. Viral whole genome sequencing

Sequencing and genomic analyses were performed as previously described [41,42]. Sequencing libraries were prepared using multiplexed amplicon panels from Swift Biosciences or Illumina COVIDSeq. Consensus sequences were assembled using a custom bioinformatics pipeline (https://github.com/greninger-lab/covid_swift_pipeline,[42]). Phylogenetic lineage was assigned using the PANGOLIN (Phylogenetic Assignment of Named Global Outbreak LINeages, https://pangolin.cog-uk.io/) and NextClade (https://clades.nextstrain.org/) tools.

3.3. RT-ddPCR

RT-ddPCR was carried out using the One-Step RT-ddPCR Advanced Kit for Probes and Automated Droplet Generation Oil for Probes (Bio-Rad) according to manufacturer instructions and as previously described [36]. Each specimen was used in three reactions, using the primers and probes in Table 1. Reference Specimens (Supplement 1) were included as positive controls in each run. Data analysis was conducted with QuantaSoft Pro 1.0.596 version software, using two methods. First, mutation identification: designating all assays as Amplitude Multiplex (Table 2), using 2D amplitude of positive controls as guides for cluster selection, as in Fig. 2. (Note that droplets are colored for ease of visualization.) For each reaction, the allele with the most droplets (at least 5–10x that of the next allele) was identified as the allele for that specimen. Second, droplet amplitudes: designating all assays as Simplex/Duplex and selecting all droplets other than empty (water) droplets as expressing all probes, then exporting all Cluster Data to Excel. In both analysis methods, samples were only included if they had a minimum of 10,000 measured droplets and a minimum of 3 droplets in a cluster.

Table 1
Primer and Probe Sequences for RT-ddPCR assays. Each assay is identified by the amino acid(s) in Spike RBD it targets. For each probe name, bold letters indicate the amino acid detected by that probe. For each probe sequence, bold/underlined letters indicate the mutation that results in the amino acid change. Primer and probe sequences for 501Y are the same as the S1B set listed in [36].

Reaction	Primer/Probe Name	Sequence
417	S417Forward	GAGGTGATGAAGTCAGACAAATCG
	S417Reverse	GCAGCCTGTAAAATCATCTGGTAA
	S417**N**Probe	**FAM**_CTGGAAA**T**ATTGCTGATTAT_**MGB**
	S417**T**Probe	**VIC**_CTGGAACGATTGCTG_**MGB**
484	S484Forward	TTAGGAAGTCTAATCTCAAACCTTTTGAG
	S484Reverse	CTGTATGGTTGGTAACCAACACCAT
	S484**K**Probe	**FAM**_CCTT**T**AACACCATTACAAGGT_**MGB**
	S484**E**Probe	**VIC**_CCTTCAACACCATTACAAGG_**MGB**
452/501	S452Forward	CAATCTTGATTCTAAGGTTGGTGGTA
	S452Reverse	CGGCCTGATAGATTTCAGTTGAA
	S452**R**Probe	**FAM**_ACCGGTATAGATTGTTTAGGAA_**MGB**
	S501Forward	ATGGTGTTGAAGGTTTTAATTGTTACTTT
	S501Reverse	GTGCATGTAGAAGTTCAAAAGAAAGTACTA
	S501**Y**Probe	**VIC**_ATGGTTTCCAACCCACT**T**AT_**MGB**

Abbreviations: FAM, 6-carboxyfluorescein; MGB, Minor Groove Binder; VIC, 2′-chloro-7′-phenyl-1,4-dichloro-6-carboxy-fluoroscein.

Table 2
QuantaSoft analysis settings for RT-ddPCR assays. To identify alleles in RT-ddPCR results, the assay type Amplitude Multiplex was selected with allele identifiers for each reaction.

	Reaction		
Signal	417	484	452/501
FAM Lo	K417	E484Q	L452
FAM Hi	K417N	E484K	L452R
VIC Lo	K417T	E484	N501
VIC Hi	–	–	N501Y

3.4. Clinical specimens

Reference Specimens: Four lineages were selected to represent the amino acids present at the time in the targeted RBD sites (Table 3). Four high-concentration specimens from each lineage were identified in the UWVL SARS-CoV-2 repository based on Whole Genome sequencing (WGS) results. One of each lineage was diluted in PBS into ~5000 copies/µl extraction controls, and extracted RNA from all were made into 1:10 serial dilutions in water for RT-ddPCR controls (Supplement 2).

Validation Specimens gathered from UWVL: 419 SARS-CoV-2-positive clinical specimens collected between 1/29/2021 and 6/17/2021; 16 SARS-CoV-2-negative clinical specimens (8 each collected in PBS and UTM); and 24 samples positive for other respiratory viruses.

Omicron Specimens: From 11/29/21 to 12/8/21, 2657 positive

Table 3
Amino acids at RBD sites in each control lineage used. [1]Omicron (BA.x) is included for comparison, but had not yet been identified during initial validation of the assay. [2]Omicron has the N501Y change, but also has additional mutations within the probe site (G496S and Q498R in BA.1, Q498R in other subvariants) that reduce fluorescence amplitude.

	Amino acid target			
Lineage	417	452	484	501
D614G	K	L	E	N
Beta	N	L	K	Y
Gamma	T	L	K	Y
Kappa	K	R	Q	N
BA.1/BA.2[1]	N	L	K	Y[2]
BA.4/BA.5[1]	N	R	K	Y[2]

clinical specimens were screened by TaqPath assay as previously described [36]. Sixteen of these were identified as S-gene dropouts and were tested in the RT-ddPCR assay.

This study was approved under a waiver of consent by the University of Washington institutional review board. GISAD IDs for all specimens are listed in Supplement 1.

4. Results

4.1. How the assay works

Droplet digital (dd)PCR reactions take place inside oil-separated droplets, using TaqMan probe detection: when a probe is bound to the template, amplification separates the dye on the 5′ end from the quencher on the 3′ end of the probe, releasing fluorescence. However, when the probe binds poorly to the template because of differences in probe and template sequence, the dye is cleaved less frequently and less fluorescence is released inside that droplet. At the end of the PCR reaction, the fluorescence within each droplet is measured. The amplitude (brightness) of fluorescence within each droplet indicates how well the probe bound to the template and therefore can be used to determine the mutation state of that template.

We selected one concentration of each control, ~Ct 28–30, where each droplet contained at most one copy of template. We measured the amplitude of all non-empty droplets from each specimen and determined that all alleles were clearly identifiable with three combinations of primers and probes (Fig. 1).

4.2. Template concentration range

To confirm that extra copies of template do not increase fluorescence amplitude within a droplet, we tested the complete dilution series of all controls, and compared amplitudes (Fig. 2, Supplement 2). RT-ddPCR assays contain 10k+ droplets each, so template concentration ranged from 1 to >50 copies per droplet. Increased concentration did in some cases change amplitude (e.g., 417 N and 452R), but these were still readily distinguishable from high- and low-concentration amplitudes from other mutations.

We determined a rough lower limit of detection (LoD) using serial 10-fold dilutions of one specimen per mutation, with four replicates per concentration (Table 4). Each dilution was also measured in RT-PCR in duplicate. Higher template concentrations were necessary to obtain at least 3 positive droplets for mismatch alleles (i.e., 417 K and 484Q), but for the targets definitively identified by a probe, lower LoD ranged from 6.5 to 14 copies / reaction.

4.3. Accuracy

We tested 390 additional clinical specimens with the assay, and ddPCR mutation determination for 99.0% of detected samples agree with WGS (Table 5, Supplement 1).

During the course of testing, we found two additional mutations that affected droplet amplitude. A search of all UWVL sequences in GISAID conducted in late July 2021 showed that these were the only two mutations in probe regions that occurred at greater than 1% frequency. Both happened to be synonymous mutations within the codon for the mutation of interest for that probe (Fig. 3). In the 484E probe, 1.1% of Alpha sequences included GAG instead of GAA (Fig. 3A), resulting in a reduction in amplitude that was still easily distinguishable from CAA (Q) or AAA (K). In the 417T probe, 4.0% of Gamma sequences included ACA instead of ACG (Fig. 3B), resulting in amplitude almost indistinguishable from AAG (K). A search of GISAID completed on 12/14/2021

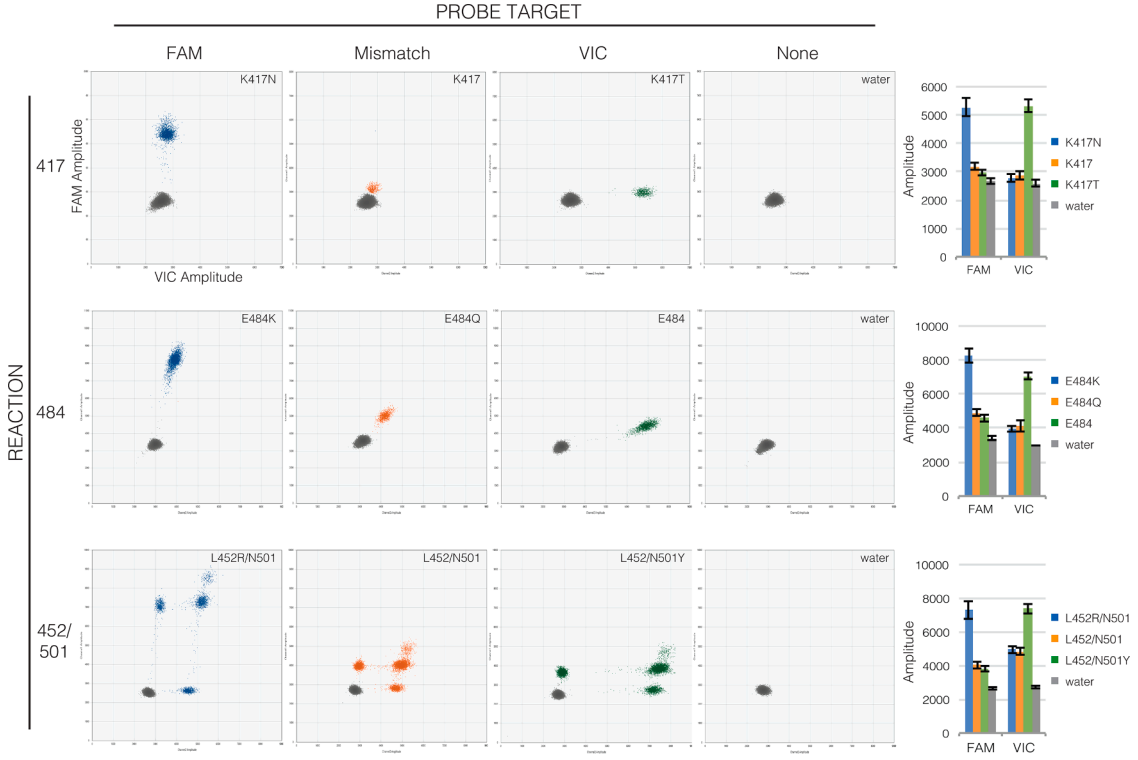

Fig. 1. Probe binding clearly distinguishes mutations in RT-ddPCR. Droplet amplitude plots ($n = 1$ per allele) illustrate how FAM fluorescence (X axis) and VIC fluorescence (Y axis) are diagnostic of templates matching the FAM probe (first column, blue droplets) or VIC probe (third column, green droplets) compared to templates with mutations in probe sequences (second column, orange droplets) and to droplets that lack template (fourth column, grey droplets) for each reaction (rows). Bar graphs (final column) show the consistency of amplitudes between specimens (average mean amplitude ± average standard deviation of 190–1900 positive droplets each, $n = 4$ per allele). Note that in the 452/501 reaction, unlike the 417 and 484 reactions, the two probes have separate targets so droplets may show fluorescence from only one or the other target (droplets lower along the axes) or from both targets (droplets higher along the axes).

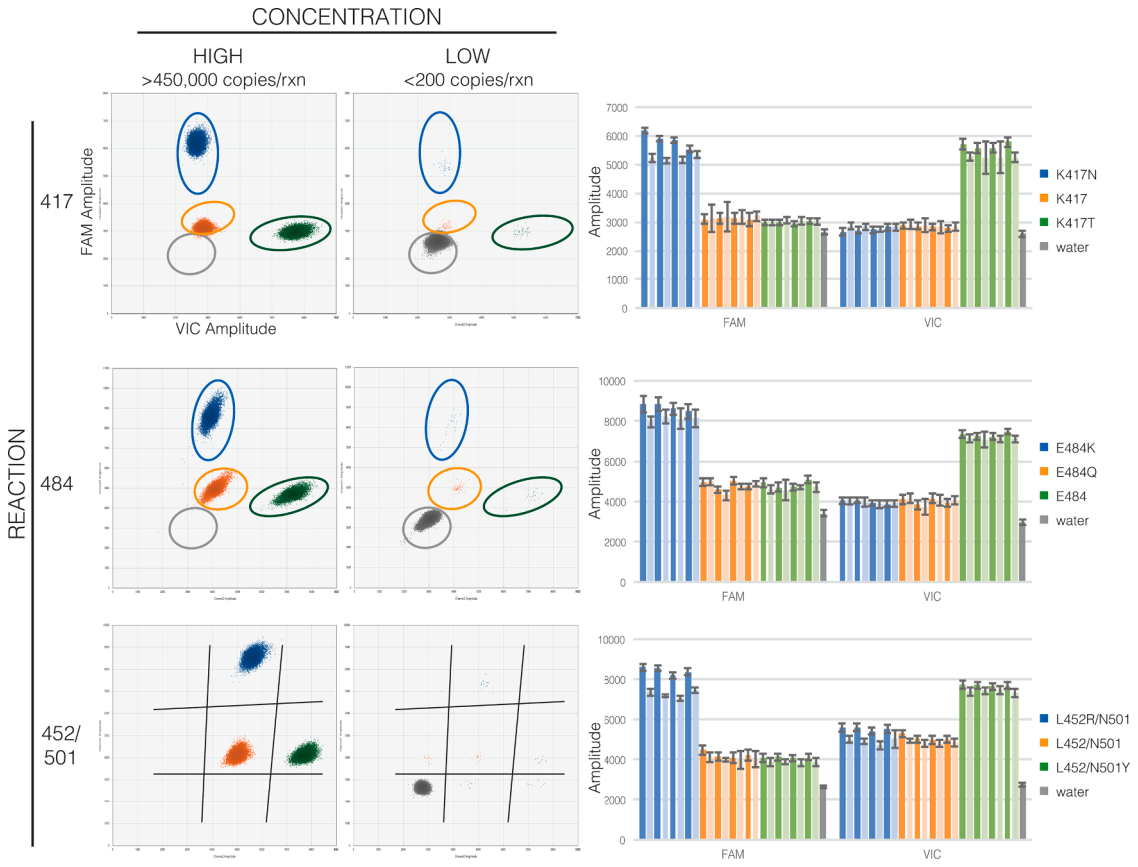

Fig. 2. Template concentration does not affect assay accuracy. For each reaction (rows), composite droplet amplitude plots showing the highest-concentration sample of each allele (first column) and lowest-concentration dilution with >10 positive droplets of the same samples (second column) illustrate that amplitudes are diagnostic of template sequences despite wide differences in copy number per droplet. Circles or lines separating droplets from different alleles are for reference on the low-concentration plots. Bar graphs (final column) show this is consistent between specimens (mean amplitude ± standard deviation of highest [dark] and lowest [light] concentration of each specimen, $n = 4$ per allele).

Table 4
Rough Limit of Detection (LoD) for each RT-ddPCR reaction. Dilutions were measured in quadruplicate in RT-ddPCR and in duplicate in RT-PCR (using primer/probe set from [43] as described in [44]). Targets with mismatches to both FAM and VIC probes are indicated with blue type. Mean concentrations are those measured in RT-ddPCR replicates at the LoD; for the dilution beyond LoD (gray type), concentrations are calculated from the LoD.

Reaction	Amino acid(s)	E Ct	Mean copies/ µL	Mean copies/ Rxn	Positive replicates	
417	K	33.4	2.22	22.2	4/4	At LoD
	N	35.7	0.77	7.7	4/4	
	T	35.1	1.39	13.9	4/4	
	K	37.1	0.22	2.2	1/4	Beyond
	N	37.3	0.07	0.8	0/4	LoD
	T	NDET	0.14	1.4	0/4	
484	E	33.4	0.65	6.5	4/4	At LoD
	K	35.1	0.88	8.8	4/4	
	Q	30.8	13.10	131.0	4/4	
	E	37.1	0.07	0.7	0/4	Beyond
	K	NDET	0.09	0.9	0/4	LoD
	Q	34.1	1.31	13.1	3/4	
452/ 501	L/N	33.4	1.17	11.7	4/4	At LoD
	L/Y	35.1	0.86	8.6	4/4	
	R/N	34.1	0.91	9.1	4/4	
	L/N	37.1	0.11	1.2	1/4	Beyond
	L/Y	NDET	0.09	0.9	0/4	LoD
	R/N	NDET	0.09	0.9	2/4	

(Supplement 3) revealed that even though UWVL deposited only a tiny percentage of Spike_K417T sequences (Fig. 3C), this mutation was greatly enriched in samples sequenced by UWVL, but its presence lasted only a little over a month (Fig. 3D).

4.4. Collection media equivalency and specificity

Negative clinical specimens collected in PBS and in VTM were analyzed alone and with 1/100 spike of extraction controls. All negative samples were undetected with the assay, all spiked samples were identified accurately, and collection medium did not affect measured concentration (Table 6).

To measure cross-reactivity, RNA from 24 individual specimens with high copy number of 10 different respiratory viruses, including adenovirus (AdV), bocavirus (BoV), two other human coronaviruses, influenza A (IAV), metapneumovirus (MPV), parainfluenzavirus 1 and 4 (PIV1, PIV4), rhinovirus (RhV), and respiratory syncytial virus (RSV) were analyzed using the assay. To measure microbial interference, these RNA samples were spiked with 1/100 dilution of each mutation control. No amplification of other viruses was detected, and the presence of those viruses did not affect the accuracy of mutation determination for spiked-in controls (Table 6).

4.5. Accurate identification of Omicron from SGTF specimens

Between November 29 and December 8, 2021, we tested 2657 SARS-CoV-2 positive clinical specimens by TaqPath assay, with 16 clear SGTF results. These 16 specimens were tested by the RT-ddPCR assay along

Table 5
Comparison of RT-ddPCR and WGS results for clinical specimens at each of four amino acids. The number of specimens with a given genotype based on RT-ddPCR (rows) and WGS (columns) is listed for each assay. For each mutation, the Positive Predictive Value (PPV) and Negative Predictive Value (NPV) are calculated based on this comparison.

		WGS 417K	417N	417T	Total			WGS 484E	484K	484Q	Total
ddPCR	417K	359	0	2	361	ddPCR	484E	322	0	0	322
	417N	0	23	0	23		484K	1	79	0	80
	417T	0	0	35	35		484Q	0	0	17	17
	Total	359	23	37	419		Total	323	79	17	419
		PPV:	100	100				PPV:	100	100	
		NPV:	100	99.5				NPV:	99.7	100	

		WGS 452L	452R	Total			WGS 501N	501Y	Total
ddPCR	452L	319	0	319	ddPCR	501N	149	0	149
	452R	0	100	100		501Y	2	268	270
	Total	319	100	419		Total	151	268	419
		PPV:	100				PPV:	99.3	
		NPV:	100				NPV:	98.7	

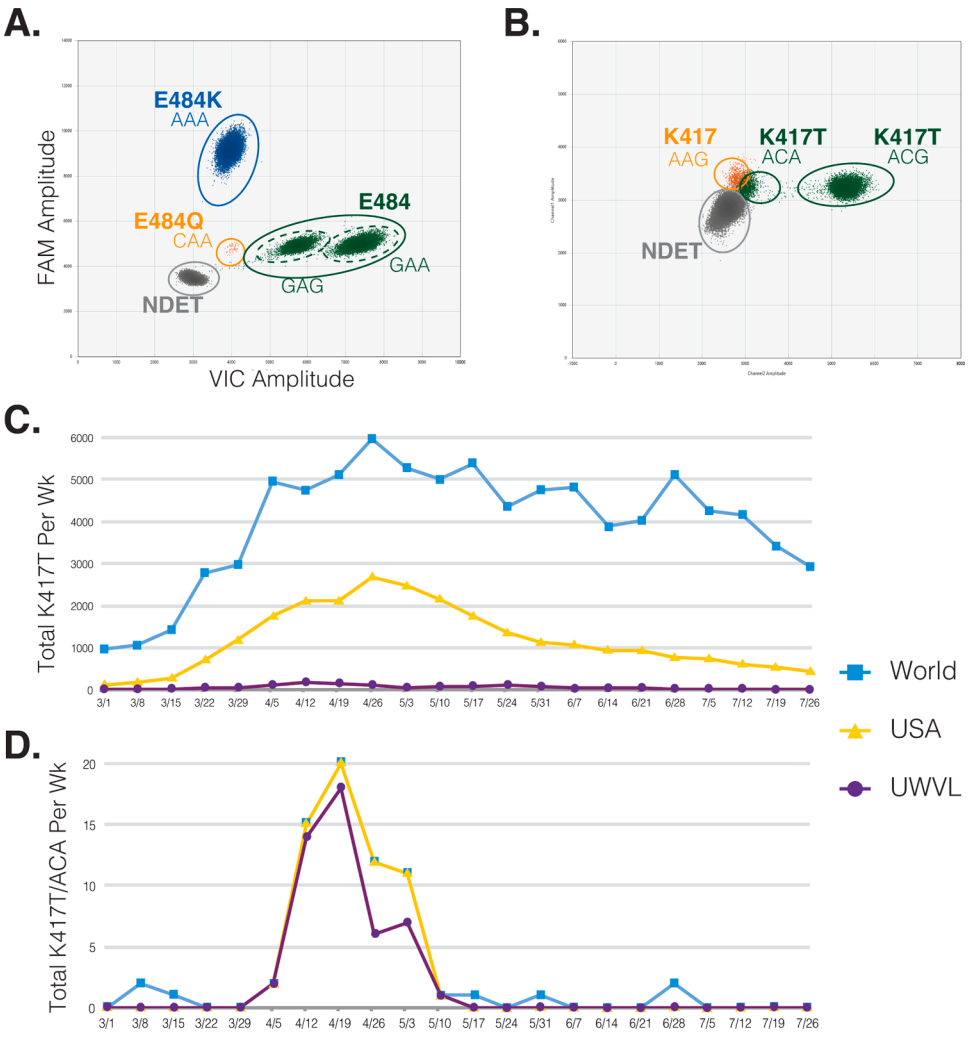

Fig. 3. Additional UWVL-identified mutations in probe sequence have variable effects on assay accuracy. (A) Mutation A->*G* in Spike_E484 results in decreased droplet amplitude that is still distinguishable from other alleles. (B) Mutation G->*A* in Spike_K417T results in decreased amplitude that is barely distinguishable from K417. (C-D) K417T sequences from samples collected within the week beginning each listed date in the world as a whole, the USA as a whole, or by UWVL: (C) total K417T sequences; (D) sequences with K417T encoded by ACA instead of ACG codon.

with five non-SGTF specimens (Fig. 4). All non-SGTF specimens were clearly Delta. The first SGTF was identified as Delta, and the subsequent 15 were identified as not-Delta, with a combination of droplet amplitudes that matched published sequences for Omicron (Supplement 3): K417N; L452; and mutations in the regions of both 484 and 501 that we had not seen in any previous variants. Whole genome sequencing confirmed the identification of all 16 SGTF specimens: one Delta with the 69–70 deletion associated with SGTF; and 15 Omicron with E484A and G496S/Q498R/N501Y.

Table 6
RT-ddPCR reactions are specific for SARS-CoV-2. Sixteen SARS-CoV-2-negative clinical specimens and 24 specimens positive for additional respiratory viruses were tested both alone and with spiked-in RNA from each allele in all assay reactions. Allele determinations were made based on droplet amplitudes.

		Virus Tested								
	Accession #s	AdV SC7118	BoV SC5484 SC7321	CoV: HKU1 SC5834 SC5875 SC5891 SC5934 SC5982 SC6302	CoV: NL63 SC5641 SC5968 SC6107 SC6263	IAV SC5416 SC5539	MPV SC5403 SC5517	PIV1 SC5381	PIV4 SC5375 SC6346	RhV SC5360 SC5382
Spike Tested	None	–	–	–	–	–	–	–	–	–
	417K	K	K	K	K	K	K	K	K	K
	417N	N	N	N	N	N	N	N	N	N
	417T	T	T	T	T	T	T	T	T	T
	None	–	–	–	–	–	–	–	–	–
	484E	E	E	E	E	E	E	E	E	E
	484K	K	K	K	K	K	K	K	K	K
	484Q	Q	Q	Q	Q	Q	Q	Q	Q	Q
	None	–	–	–	–	–	–	–	–	–
	452L	L	L	L	L	L	L	L	L	L
	452R	R	R	R	R	R	R	R	R	R
	None	–	–	–	–	–	–	–	–	–
	501N	N	N	N	N	N	N	N	N	N
	501Y	Y	Y	Y	Y	Y	Y	Y	Y	Y

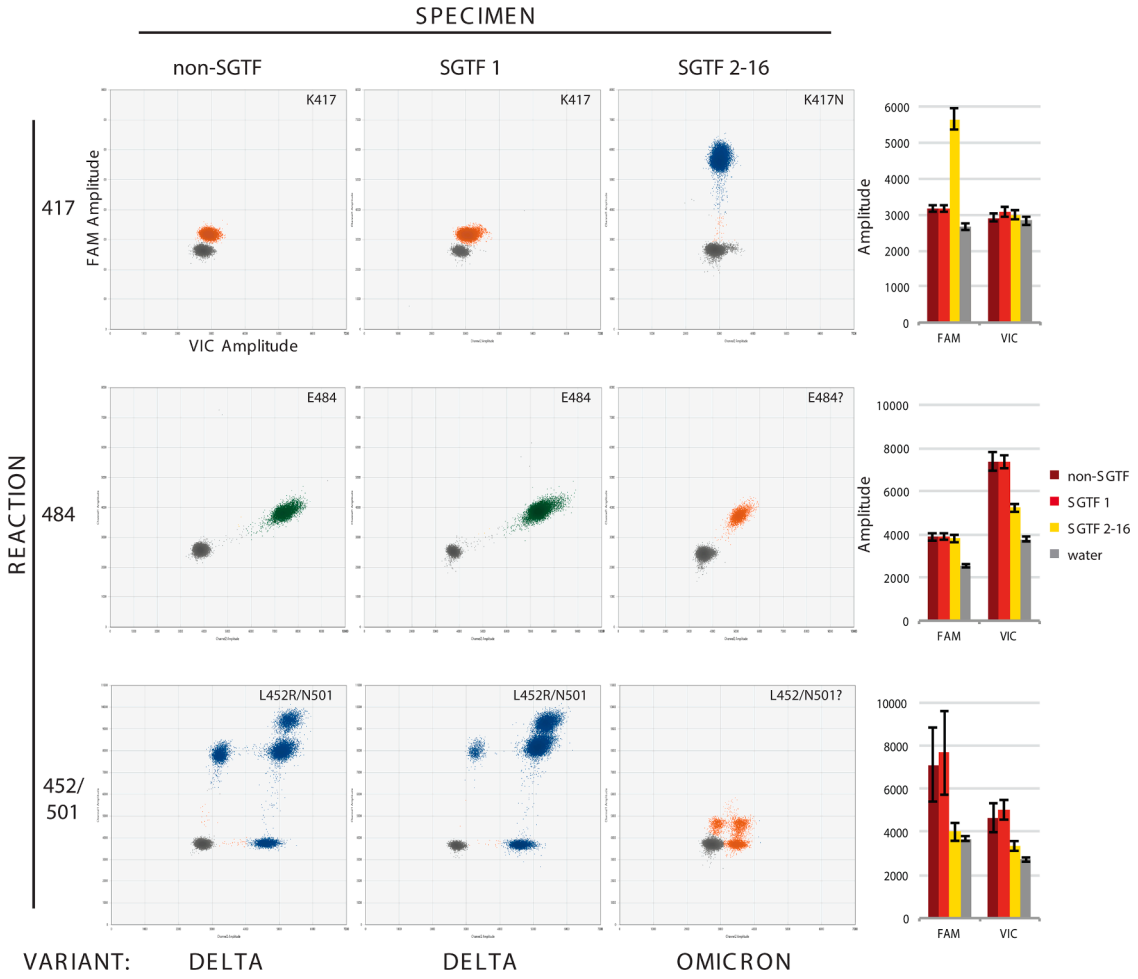

Fig. 4. Omicron specimens are accurately identified with the assay. Droplet amplitude plots ($n = 1$ per specimen type) illustrate the different assay results for three categories of newly-collected specimen: non-SGTF (first column), the first SGTF identified at UWVL (second column), and all subsequent SGTF (third column) for each reaction (rows). Bar graphs (final column) show average mean amplitude (± average standard deviation) for samples from each category ($n = 5$, $n = 1$, and $n = 7$ respectively). Variant determination (bottom) based on the assay was confirmed in all cases by whole-genome sequencing.

5. Discussion

Through the spring and summer of 2021, numerous SARS-CoV-2 VOC appeared and spread and changed in frequency across the globe in a way that complicated efforts by public health professionals. Some of the mutations carried by these variants were associated with increased transmissibility, which was of concern to those working to contain the epidemic. Others were associated with significant immune evasion, which was of great concern to doctors looking to treat vulnerable COVID-19 patients with monoclonal antibodies, some of the only drugs

available for combatting SARS-CoV-2 at the time [23,24] .

When the Delta variant overtook all other variants, accounting for over 99% of all cases sequenced by UWVL by 8/22/21, it was tempting to think that the need to rapidly identify variants had ended. Certainly, the complexity of mAb selection decisions appeared to be reduced. But as the emergence and rapid spread of the Omicron variant demonstrates, viral evolution continues and so does our need to track it.

Omicron was first identified in late November 2021, with a substantial number of mutations in Spike from pre-Delta variants [31,45]: K417N, N501Y, a change at E484 (E484A), and an impressive number of novel mutations. In the months since Omicron first appeared, its lineage has continued to evolve: BA.1 was replaced by BA.2, which is now being replaced by BA.4 and BA.5 that both carry the L452R mutation from Delta. Some of these mutations are correlated with substantial reduction in the efficacy of endogenous as well as many mAbs [46–49]. Sotrovimab and related mAbs largely retained the ability to neutralize B.1.1.529/BA.1 [32,49], but BA.2 evades even sotrovimab [50]. Once again, clinicians may need to identify variant before prescribing mAbs for their patients, and once again this is a task that must be accomplished rapidly in order for mAb treatment to be effective in preventing severe disease.

Because this RT-ddPCR assay targets the sequences directly related to the antigen escape of SARS-CoV-2 variants, and does so rapidly, it is a useful tool for clinical decision-making. Its use can also allow limited public health resources for case tracking and tracing to be focused on mutations/variants of greater concern. Rapid variant identification can also allow selection of specimens for scientific analysis without the delay and added expense of whole genome sequencing. For example, use of this assay in March and August of 2021 allowed us to rapidly select Alpha, Epsilon, and Delta variant samples [11], enabling a comparison of variant growth in culture that would have been much more tenuous if the specimens needed to be held for sequencing (either subjected to lengthy storage at 4 °C or to additional freeze-thaw cycles) before selection. It also allowed us to identify two specimens as Delta-Omicron coinfections, rather than novel variants [51].

The utility of the assay is limited by several factors. First, while ddPCR technology has many uses beyond this particular assay in our laboratory, (e.g., [44,52–54]), it is not widely available in clinical settings. Second, as the example of ACG→ACA mutation in K417T illustrates, assay accuracy is subject to change with additional mutations as for all PCR-based genotyping methods. Third, while the direct targeting of mutations of concern for mAb escape increases the chances that the assay will continue to be useful for future variants (as has been the case with Delta, B.1.1.529/BA.1, and BA.4/BA.5), there is no guarantee that this will always be the case. For example, only a single nucleotide each distinguishes BA.1 and BA.2.12.1 from other subvariants within the probe sites for this assay: BA.1 has G496S (AGT) while others have G496 (GGT); BA.2.12.1 has L452Q (CAG) while BA.1/BA.2 have L452 (CTG) and BA.4/BA.5 have L452R (CGG). The latter likely results in a functional but undetectable change, since the probe is designed to recognize CGG; the former is likely a detectable change that is unlikely to explain BA.2 antigen escape. Reliance on non-causative changes like G496S or the 69–70 deletion increases the chances of false positives (as in the case of the SGTF-Delta specimen we identified) or false negatives (as in the case of BA.2 which lacks the 69–70 deletion [55]).

We have previously used RT-ddPCR to identify SARS-CoV-2 Alpha variant in clinical specimens, but here we expand both the number of lineages that can be tracked with the assay and our understanding of the assay robustness. It can accommodate a wide range of sample concentrations, coinfections, and other confounds, and still yield an accurate determination of SARS-CoV-2 mutations quickly enough to enable clinical decision-making.

Declaration of Competing Interest

A.L.G. and K.R.J. report contract testing from Abbot and A.L.G. research support from Merck and Gilead.The other authors declare no conflicts of interest.

Acknowledgements

We gratefully acknowledge all the laboratories around the world involved in the generation and deposition of SARS-CoV-2 sequence data that we obtained from GISAID (Supplement 3).

This research did not receive any specific grant from funding agencies in the public, commercial, or not-for-profit sectors.

Supplementary materials

Supplementary material associated with this article can be found, in the online version, at doi:https://doi.org/10.1016/j.jcv.2022.105218.

References

[1] H. Othman, Z. Bouslama, J.-.T. Brandenburg, J. da Rocha, Y. Hamdi, K. Ghedira, et al., Interaction of the spike protein RBD from SARS-CoV-2 with ACE2: similarity with SARS-CoV, hot-spot analysis and the effect of the receptor polymorphism, Biochem. Biophys. Res. Commun. 527 (2020) 702–708, https://doi.org/10.1016/j.bbrc.2020.05.028&domain=pdf.

[2] J. Lan, J. Ge, J. Yu, S. Shan, H. Zhou, S. Fan, et al., Structure of the SARS-CoV-2 spike receptor-binding domain bound to the ACE2 receptor, Nature 581 (2020) 215–220, https://doi.org/10.1038/s41586-020-2180-5.

[3] R. Yan, Y. Zhang, Y. Guo, L. Xia, Q. Zhou, Structural basis for the recognition of the 2019-nCoV by human ACE2, bioRxiv (2020), https://doi.org/10.1101/2020.02.19.956946.

[4] L. Dai, G.F. Gao, Viral targets for vaccines against COVID-19, Nat. Rev. Immunol. 21 (2021) 73–82 (accessed December 15, 2021).

[5] A. Baum, B.O. Fulton, E. Wloga, R. Copin, K.E. Pascal, V. Russo, et al., Antibody cocktail to SARS-CoV-2 spike protein prevents rapid mutational escape seen with individual antibodies, Science 369 (2020) 1014–1018.

[6] Z. Liu, L.A. VanBlargan, L.-.M. Bloyet, P.W. Rothlauf, R.E. Chen, S. Stumpf, et al., Identification of SARS-CoV-2 spike mutations that attenuate monoclonal and serum antibody neutralization, Cell Host Microbe 29 (2021) 477–488, https://doi.org/10.1016/j.chom.2021.01.014, e4.

[7] T.N. Starr, A.J. Greaney, A. Addetia, W.W. Hannon, M.C. Choudhary, A.S. Dingens, et al., Prospective mapping of viral mutations that escape antibodies used to treat COVID-19, Science 371 (2021) 850–854.

[8] A.J. Greaney, A.N. Loes, K.H.D. Crawford, T.N. Starr, K.D. Malone, H.Y. Chu, et al., Comprehensive mapping of mutations in the SARS- CoV-2 receptor-binding domain that affect recognition by polyclonal human plasma antibodies, Cell Host Microbe 29 (2021) 463–476, https://doi.org/10.1016/j.chom.2021.02.003, e6.

[9] E. Andreano, G. Piccini, D. Licastro, L. Casalino, N.V. Johnson, I. Paciello, et al., SARS-CoV-2 escape from a highly neutralizing COVID-19 convalescent plasma, Pnas 118 (2021) 1–7, https://doi.org/10.1073/pnas.2103154118/-/DCSupplemental.

[10] Z. Wang, F. Schmidt, Y. Weisblum, F. Muecksch, C.O. Barnes, S. Finkin, et al., mRNA vaccine-elicited antibodies to SARS-CoV-2 and circulating variants, Nature (2021) 1–23, https://doi.org/10.1038/s41586-021-03324-6.

[11] H.W. Despres, M.G. Mills, D.J. Shirley, M.M. Schmidt, M.-.L. Huang, K.R. Jerome, et al., Quantitative measurement of infectious virus in SARS-CoV-2 Alpha, Delta and Epsilon variants reveals higher infectivity (viral titer:RNA ratio) in clinical samples containing the Delta and Epsilon variants, medRxiv (2021) 1–16, https://doi.org/10.1101/2021.09.07.21263229.

[12] A. Castro, H. Carter, M. Zanetti, Potential global impact of the N501Y mutation on MHC-II presentation and immune escape, bioRxiv (2021) 1–4, https://doi.org/10.1101/2021.02.02.429431.

[13] G. Iacobucci, Covid-19: new UK variant may be linked to increased death rate, early data indicate, BMJ 372 (2021) 1–2, https://doi.org/10.1136/bmj.n230.

[14] R. Challen, E. Brooks-Pollock, J.M. Read, L. Dyson, K. Tsaneva-Atanasova, L. Danon, Risk of mortality in patients infected with SARS-CoV-2 variant of concern 202012/1: matched cohort study, BMJ 372 (2021) 1–10, https://doi.org/10.1136/bmj.n579.

[15] S.A. Madhi, V. Baillie, C.L. Cutland, M. Voysey, A.L. Koen, L. Fairlie, et al., Efficacy of the ChAdOx1 nCoV-19 Covid-19 vaccine against the B.1.351 variant, New England J. Med. 384 (2021) 1–14, https://doi.org/10.1056/NEJMoa2102214.

[16] D. Zhou, W. Dejnirattisai, P. Supasa, C. Liu, A.J. Mentzer, H.M. Ginn, et al., Evidence of escape of SARS-CoV-2 variant B.1.351 from natural and vaccine-induced sera, Cell 184 (2021) 2348–2361, https://doi.org/10.1016/j.cell.2021.02.037, e6.

[17] E.C. Sabino, L.F. Buss, M.P.S. Carvalho, C.A. Prete Jr, M.A.E. Crispim, N.A. Fraiji, et al., Resurgence of COVID-19 in Manaus, Brazil, despite high seroprevalence, Lancet 397 (2021) 452–455, https://doi.org/10.1016/S0140-6736(21)00183-5.

[18] F.G. Naveca, V. Nascimento, V.C. Souza, A. de Lima Corado, F. Nascimento, G. Silva, et al., COVID-19 in Amazonas, Brazil, was driven by the persistence of endemic lineages and P.1 emergence, Nat. Med. (2021) 1–17, https://doi.org/10.1038/s41591-021-01378-7.

[19] N.R. Faria, T.A. Mellan, C. Whittaker, I.M. Claro, D.D.S. Candido, S. Mishra, et al., Genomics and epidemiology of the P.1 SARS-CoV-2 lineage in Manaus, Brazil, Science 372 (2021) 815–821, https://doi.org/10.1126/science.abh2644.
[20] A. Sheikh, J. McMenamin, B. Taylor, C. Robertson, P.H.S.A.T.E.I. Collaborators, SARS-CoV-2 Delta VOC in Scotland: demographics, risk of hospital admission, and vaccine effectiveness, The Lancet 397 (2021) 2461–2462, https://doi.org/10.1016/S0140-6736(21)01358-1.
[21] D. Planas, D. Veyer, A. Baidaliuk, I. Staropoli, F. Guivel-Benhassine, M.M. Rajah, et al., Reduced sensitivity of SARS-CoV-2 variant Delta to antibody neutralization, Nature (2021) 1–20, https://doi.org/10.1038/s41586-021-03777-9.
[22] S. Cherian, V. Potdar, S. Jadhav, P. Yadav, N. Gupta, M. Das, et al., SARS-CoV-2 Spike mutations, L452R, T478K, E484Q and P681R, in the Second Wave of COVID-19 in Maharashtra, 9, Microorganisms, India, 2021, pp. 1–11, https://doi.org/10.3390/microorganisms9071542.
[23] Y. Weisblum, F. Schmidt, F. Zhang, J. DaSilva, D. Poston, J.C.C. Lorenzi, et al., Escape from neutralizing antibodies by SARS-CoV-2 spike protein variants, Elife 9 (2020) 1–31, https://doi.org/10.7554/eLife.61312.
[24] M. Tuccori, S. Ferraro, I. Convertino, E. Cappello, G. Valdiserra, C. Blandizzi, et al., Anti-SARS-CoV-2 neutralizing monoclonal antibodies: clinical pipeline, MAbs 12 (2020) 1–9, https://doi.org/10.1080/19420862.2020.1854149.
[25] L.J. Estcourt, Passive immune therapies: another tool against COVID-19, Hematology Am. Soc. Hematol. Educ. Program 1 (2021) 628–641, https://doi.org/10.1182/hematology.2021000299, 2021.
[26] M.P. O'Brien, E. Forleo-Neto, B.J. Musser, F. Isa, K.-.C. Chan, N. Sarkar, et al., Subcutaneous REGEN-COV antibody combination to prevent Covid-19, New England J. Med. 385 (2021) 1184–1195, https://doi.org/10.1056/NEJMoa2109682.
[27] S. Reardon, Do monoclonal antibodies help COVID patients? Sci. Am. (2021).
[28] D. Coffey, Monoclonal antibodies vs. vaccines vs. COVID-19: what to know, WebMD.com (2021).
[29] S. Lusvarghi, W. Wang, R. Herrup, S.N. Neerukonda, R. Vassell, L. Bentley, et al., Key substitutions in the spike protein of SARS-CoV-2 variants can predict resistance to monoclonal antibodies, but other substitutions can modify the effects, J. Virol. (2021) 1–45, https://doi.org/10.1128/JVI.01110-21.
[30] C. Gaebler, Z. Wang, J.C.C. Lorenzi, F. Muecksch, S. Finkin, M. Tokuyama, et al., Evolution of antibody immunity to SARS-CoV-2, Nature (2021) 1–30, https://doi.org/10.1038/s41586-021-03207-w.
[31] M. Kandeel, M.E.M. Mohamed, H.M. Abd El-Lateef, K.N. Venugopala, H.S. El-Beltagi, Omicron variant genome evolution and phylogenetics, J. Med. Virol. (2021) 1–6, https://doi.org/10.1002/jmv.27515.
[32] A.L. Cathcart, C. Havenar-Daughton, F.A. Lempp, D. Ma, M.A. Schmid, M. L. Agostini, et al., The dual function monoclonal antibodies VIR-7831 and VIR-7832 demonstrate potent in vitro and in vivo activity against SARS-CoV-2, bioRxiv (2021) 1–51, https://doi.org/10.1101/2021.03.09.434607.
[33] A.L. Greninger, J.D. Bard, R.C. Colgrove, E.H. Graf, K.E. Hanson, M.K. Hayden, et al., Clinical and infection prevention applications of Severe Acute Respiratory Syndrome Coronavirus 2 genotyping: an Infectious Diseases Society of America/American Society for Microbiology consensus review document, Clin. Infect. Dis. Viewpoints (2021) 1–7, https://doi.org/10.1093/cid/ciab761.
[34] A.L. Greninger, J.D. Bard, R.C. Colgrove, E.H. Graf, K.E. Hanson, M.K. Hayden, et al., JCM.01659-21, J. Clin. Microbiol. (2021) 1–24, https://doi.org/10.1128/JCM.01659-21.
[35] K.A. Brown, J. Gubbay, J. Hopkins, S. Patel, S.A. Buchan, N. Daneman, et al., S-gene target failure as a marker of variant B.1.1.7 among SARS-CoV-2 isolates in the greater Toronto area, December 2020 to March 2021, JAMA 325 (2021) 2115–2116, https://doi.org/10.1001/jama.2021.5607.
[36] G.A. Perchetti, H. Zhu, M.G. Mills, L. Shrestha, C. Wagner, S.M. Bakhash, et al., Specific allelic discrimination of N501Y and other SARS-CoV- 2 mutations by ddPCR detects B.1.1.7 lineage in Washington State, J. Med. Virol. 93 (2021) 1–11, https://doi.org/10.1002/jmv.27155.
[37] A. Smout, F. Guarascio, C. Lin, The race is on to trace the new COVID-19 variant, Reuters.com (2021).
[38] H. Li, R. Bai, Z. Zhao, L. Tao, M. Ma, Z. Ji, et al., Application of droplet digital PCR to detect the pathogens of infectious diseases, Biosci. Rep. 38 (2018) 1–8, https://doi.org/10.1042/BSR20181170.
[39] T.F. Pinheiro-de-Oliveira, A.A. Fonseca-Júnior, M.F. Camargos, M. Laguardia-Nascimento, S. Giannattasio-Ferraz, A.C.P. Cottorello, et al., Reverse transcriptase droplet digital PCR to identify the emerging vesicular virus Senecavirus A in biological samples, Transbound. Emerg. Dis. 66 (2019) 1360–1369, https://doi.org/10.1111/tbed.13168.
[40] Y. Tong, S. Shen, H. Jiang, Z. Chen, Application of digital PCR in detecting human diseases associated gene mutation, Cell. Physiol. Biochem. 43 (2017) 1718–1730, https://doi.org/10.1159/000484035.
[41] A.L. Greninger, D.M. Zerr, X. Qin, A.L. Adler, R. Sampoleo, J.M. Kuypers, et al., Rapid metagenomic next-generation sequencing during an investigation of hospital-acquired Human Parainfluenza Virus 3 infections, J. Clin. Microbiol. 55 (2017) 177–182, https://doi.org/10.1128/JCM.01881-16.
[42] A. Addetia, M.J. Lin, V. Peddu, P. Roychoudhury, K.R. Jerome, A.L. Greninger, Sensitive recovery of complete SARS-CoV-2 genomes from clinical samples by use of Swift Biosciences' SARS-CoV-2 multiplex amplicon sequencing panel, J. Clin. Microbiol. 59 (2021) 1–4, https://doi.org/10.1128/JCM.02226-20.
[43] V.M. Corman, O. Landt, M. Kaiser, R. Molenkamp, A. Meijer, D.K. Chu, et al., Detection of 2019 novel coronavirus (2019-nCoV) by real-time RT-PCR, Eurosurveillance 25 (2020) 2431, https://doi.org/10.1183/23120541.00227-2018.
[44] E.A. Bruce, M.G. Mills, R. Sampoleo, G.A. Perchetti, M.-.L. Huang, H.W. Despres, et al., Predicting infectivity: comparing four PCR-based assays to detect culturable SARS-CoV-2 in clinical samples, EMBO Mol. Med. (2021) 1–15, https://doi.org/10.15252/emmm.202115290.
[45] S.-.J. Gao, H. Guo, G. Luo, Omicron variant (B.1.1.529) of SARS-CoV-2, a global urgent public health alert!, J. Med. Virol. (2021) 1–2, https://doi.org/10.1002/jmv.27491.
[46] A.J. Greaney, T.N. Starr, J.D. Bloom, An antibody-escape calculator for mutations to the SARS-CoV-2 receptor-binding domain, bioRxiv (2021) 1–7, https://doi.org/10.1101/2021.12.04.471236.
[47] A. Wilhelm, M. Widera, K. Grikscheit, T. Toptan, B. Schenk, C. Pallas, et al., Reduced neutralization of SARS-CoV-2 Omicron variant by vaccine sera and monoclonal antibodies, medRxiv (2021) 1–9, https://doi.org/10.1101/2021.12.07.21267432.
[48] C. Kuhlmann, C.K. Mayer, M. Claasen, T. Maponga, A.D. Sutherlan, T. Suliman, et al., Breakthrough infections with SARS-CoV-2 Omicron variant despite booster dose of mRNA vaccine, Ssrn (2021) 1–8, https://doi.org/10.2139/ssrn.3981711.
[49] J. Chen, R. Wang, N.B. Gilby, G.-.W. Wei, Omicron (B.1.1.529): infectivity, vaccine breakthrough, and antibody resistance, arXiv (2021) 1–12.
[50] S. Iketani, L. Liu, Y. Guo, L. Liu, J.F.W. Chan, Y. Huang, et al., Antibody evasion properties of SARS-CoV-2 Omicron sublineages, Nature 604 (2022) 553–556, https://doi.org/10.1038/s41586-022-04594-4.
[51] P. Roychoudhury, S. Luo, K. Hayashibara, P. Hajian, M.G. Mills, J. Lozach, et al., Identification of Omicron-Delta coinfections using PCR-based genotyping, Microbiol. Spectr. (2022) 1–4, https://doi.org/10.1128/spectrum.00605-22.
[52] R.H. Sedlak, L. Cook, M.-.L. Huang, A. Magaret, D.M. Zerr, M. Boeckh, et al., Identification of chromosomally integrated human herpesvirus 6 by droplet digital PCR, Clin. Chem. 60 (2014) 765–772, https://doi.org/10.1373/clinchem.2013.217240.
[53] C.N. Levy, S.M. Hughes, P. Roychoudhury, D.B. Reeves, C. Amstuz, H. Zhu, et al., A highly multiplexed droplet digital PCR assay to measure the intact HIV-1 proviral reservoir, Cell Rep. Med. 2 (2021), 100243, https://doi.org/10.1016/j.xcrm.2021.100243.
[54] G.A. Perchetti, M.-.L. Huang, M.G. Mills, K.R. Jerome, A.L. Greninger, Analytical sensitivity of the Abbott BinaxNOW COVID-19 Ag card, J. Clin. Microbiol. 59 (2021) 1–8, https://doi.org/10.1128/JCM.02880-20.
[55] I. Sample, P. Walker, Scientists find "stealth" version of Omicron that may be harder to track, Guardian (2021).